

S.D. Pirozzi, B.S.¹, A.S. Nelson, M.D.¹, A.D. Nelson, Ph.D.¹, J.W. Piper, B.S.¹, B.J. Traugher, M.D.², P.F. Faulhaber, M.D.², J.K. O'Donnell, M.D.², P.F. Wojtylak, CNMT²

¹ MIM Software Inc., Cleveland, OH • ² University Hospitals Case Medical Center, Cleveland, OH

Purpose & Objectives

Various software packages have been developed for gated myocardial perfusion SPECT that use different algorithms for segmenting the left ventricle and calculating left ventricular end-diastolic and systolic volumes (EDV and ESV, respectively) and left ventricular ejection fractions (LVEF). In this study we sought to compare the left ventricular parameters for QGS, 4D-MSPECT, and MIMcardiac.

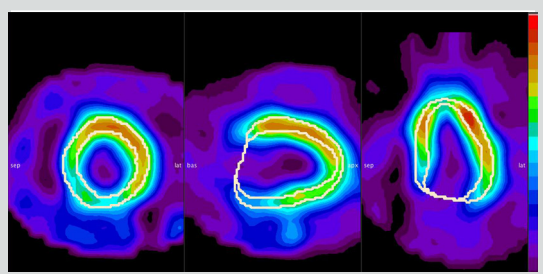
Methods & Materials

SPECT scans for 19 patients (11 males, 9 females; age range, 34-84) were randomly selected retrospectively and processed with QGS, 4D-MSPECT, and MIMcardiac. EF, EDV, and ESV were recorded and mean values and correlations (CC) between the methods were calculated.

Results

LVEF results were significantly different between all methods ($p < 0.05$) with a mean LVEF for MIMcardiac, QGS, and 4D-MSPECT of 53% +/- 6%, 60% +/- 9%, and 64% +/- 10% respectively. However, all methods were found to correlate well with CC for MIM vs QGS (0.75), MIM vs 4D-MSPECT (0.75), and QGS vs 4D-MSPECT (0.77). EDV and ESV results were also significantly different for all methods except the ESV for QGS vs 4D-MSPECT ($p=0.49$). However, volumes for all methods correlated well ($CC > 0.91$). Mean EDV and ESV for MIM, QGS, and 4D-MSPECT were (120 +/- 28ml and 57 +/- 18ml), (87 +/- 25ml and 36 +/- 18ml), and (94 +/- 25ml and 35 +/- 18ml) respectively.

Figure 2
Affine Alignment to Template Prior to Deformation



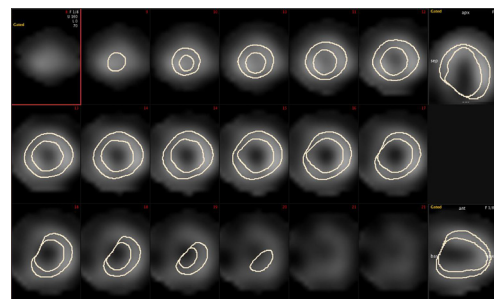
First, an affine registration is performed to scale, rotate, and translate the patient image to match the template. Next, a deformable registration is performed to refine the alignment by accounting for non-rigid differences between the patient and the template.

Figure 1

Segmentation Methods and Results for MIMcardiac, QGS, and 4D-MSPECT Results for patient where EF values differed from 5 to 10 percent between the three systems

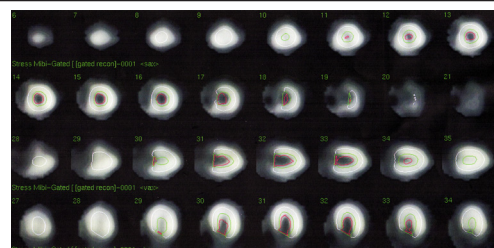
MIMcardiac

MIMcardiac uses deformable image registration and atlas-based segmentation to generate left ventricular myocardial contours. Patient images are deformed to match the size, shape, and orientation of the atlas template. Using this same deformation, contours are transformed from the template back to the original patient image. The atlas myocardial contours and valve plane deformed to the patient were defined manually on a CCTA image.



QGS

QGS locates the maximal-count midmyocardial surface using thresholding and clustering. Rays are sampled normal to this surface and count profiles are obtained for each ray. Endocardial and epicardial contours are estimated using an asymmetric gaussian fit of the count profiles (Schaefer et al., 2004). The limits for the valve plane are derived by assuming the septal wall is shorter than the lateral wall and independently estimating the basal limit for each side of the LV (Lin et al. 2006).



4D-MSPECT

4D-MSPECT derives initial estimates for the LV using a 2-dimensional gradient image. A series of 1D and 2D weighted splines are used to refine the estimated endocardial and epicardial surfaces (Schaefer et al., 2004). The basal limits are assumed to be the same in the septal and lateral walls although this can be over-ridden by the user (Lin et al 2006).

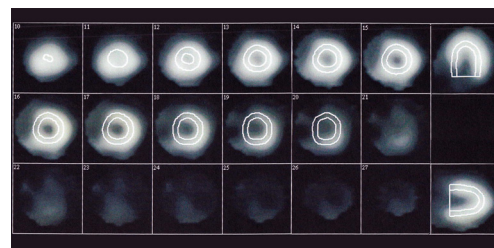


Table 1
Comparison of Left Ventricular Functional Parameters

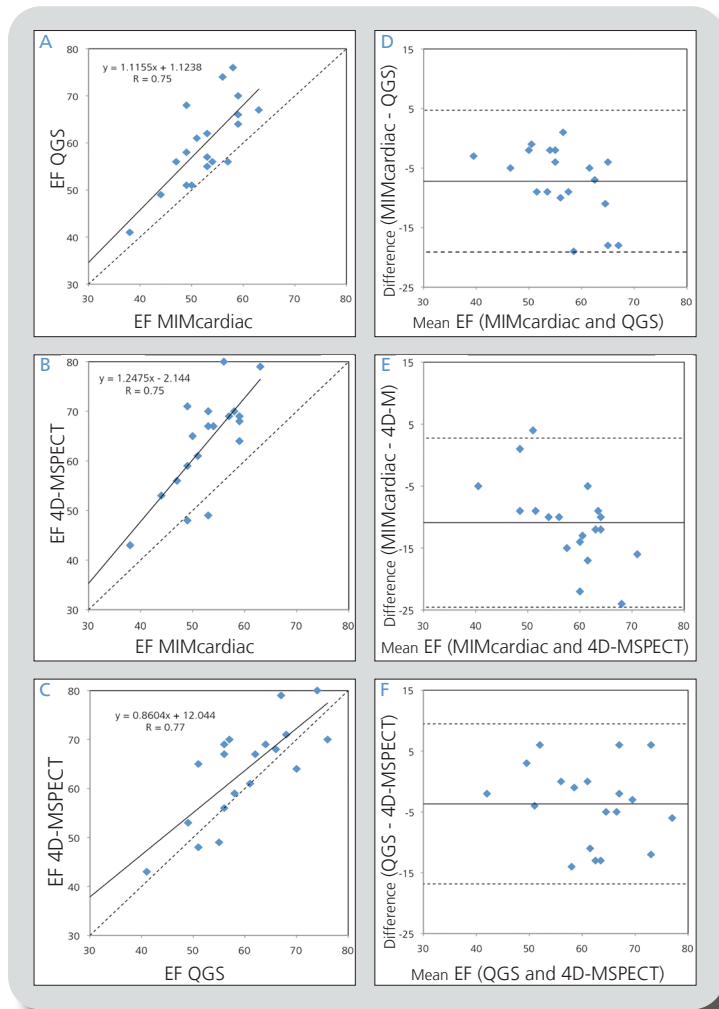
	EF			EDV			ESV		
	MIM	QGS	4D-MSPECT	MIM	QGS	4D-MSPECT	MIM	QGS	4D-MSPECT
Mean ± SD	53 ± 6	60 ± 9	64 ± 10	120 ± 28	87 ± 25	94 ± 25	57 ± 18	36 ± 18*	35 ± 18*
Range	38-63	41-76	43-80	81-173	57-140	59-147	33-106	20-82	18-75

*All results were significantly different (p -value < 0.03) except for ESV between QGS and 4D-MSPECT (p -value = 0.49).

Conclusions

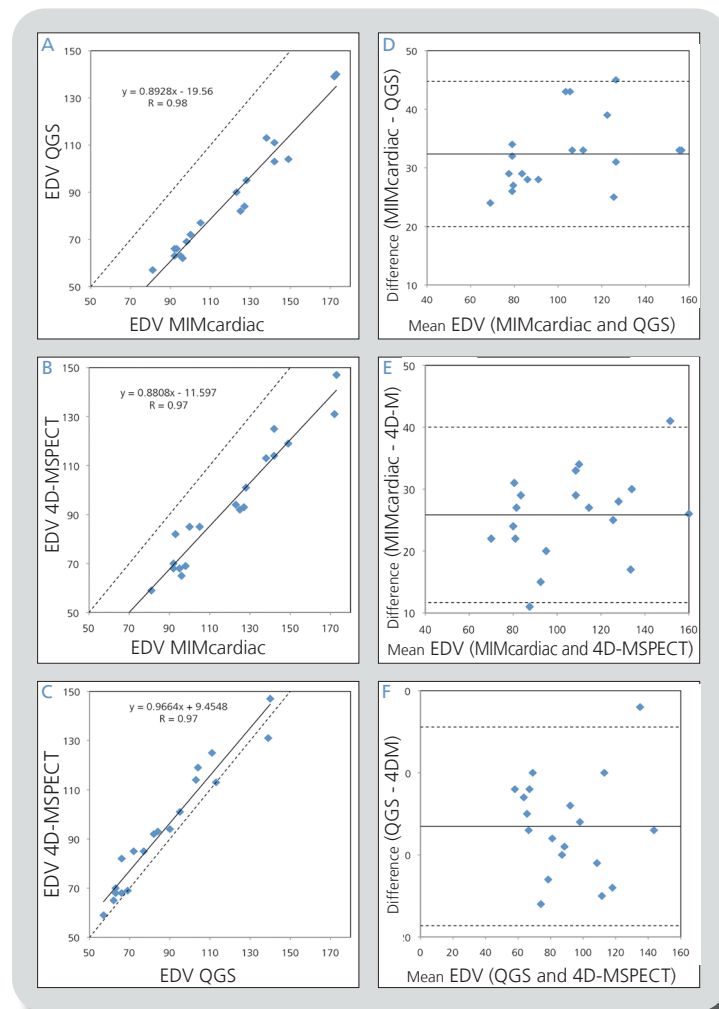
While the results for QGS, 4D-MSPECT, and MIMcardiac correlated well, the mean LVEF and LV volumes were found to differ significantly between all methods and should not be used interchangeably.

Figure 3
EF



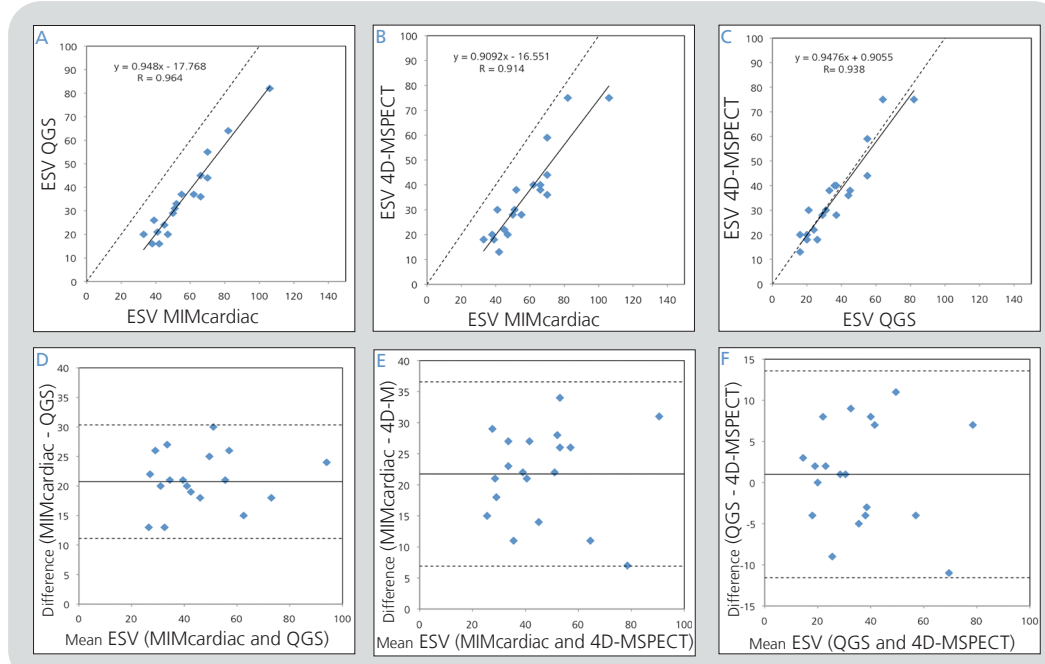
Correlation analysis of EF results between MIMcardiac and QGS (A), MIMcardiac and 4D-MSPECT (B), and QGS and 4D-MSPECT (C). Bland-Altman plots compare MIMcardiac and QGS (D), MIMcardiac and 4D-MSPECT (E), and QGS and 4D-MSPECT (F).

Figure 4
EDV



Correlation analysis of EDV results between MIMcardiac and QGS (A), MIMcardiac and 4D-MSPECT (B), and QGS and 4D-MSPECT (C). Bland-Altman plots compare MIMcardiac and QGS (D), MIMcardiac and 4D-MSPECT (E), and QGS and 4D-MSPECT (F).

Figure 5
ESV



Correlation analysis of ESV results between MIMcardiac and QGS (A), MIMcardiac and 4D-MSPECT (B), and QGS and 4D-MSPECT (C). Bland-Altman plots compare MIMcardiac and QGS (D), MIMcardiac and 4D-MSPECT (E), and QGS and 4D-MSPECT (F).

References

1. Lin G, Hines H, Grant G et al. Automated Quantification of Myocardial Ischemia and Wall Motion Defects by Use of Cardiac SPECT Polar Mapping and 4-Dimensional Surface Rendering. *Journal of Nuclear Medicine Technology* 2006; 34: 3-17.
2. Schaefer W, Lipke C, Nowak B et al. Validation of QGS and 4D-MSPECT for Quantification of Left Ventricular Volumes and Ejection Fraction from Gated 18F-FDG PET: Comparison with Cardiac MRI. *Journal of Nuclear Medicine* 2004; 45: 74-79.